DUANE C. BROWN*
DBA Systems, Inc.
Melbourne, Fla. 32901

Close-Range Camera Calibration

A photo test field consisted of a series of plumb lines whose images, because of their lack of straightness, permitted an analytical determination of lens distortion which, in addition to the usual concept, varies also with object distance.

INTRODUCTION

ONE OF THE specialized activities at DBA Systems over the last eight years has been the application of close-range photogrammetry to the very precise measurement of structures, particularly parabolic antennas. This has led to the development of a body of highly refined photogrammetric technique, the foundations of which were set in Brown (1962). The current state of this body of technique is reviewed by Kenefick (1971) in a paper scheduled for a subsequent issue. Our concern in the present paper is with one specific aspect of close-range photogrammetry, that of camera calibration. In particular, we shall be concerned with the variation of distortion within the photogrammetric model. This becomes a consideration of increasing importance as magnification increases. The essence of the problem as pointed out in Brown (1962) is as follows:

> Radial distortion is normally calibrated at infinity focus. Accuracies of ±2 microns *rms* or better for the distortion function are not difficult to obtain from a rigorous stellar calibration. . . However, optical ray tracing theory tells us that Gaussian radial distortion is a function of object distance. Thus when the focal plane is set for a sensibly finite object distance, it is necessary to employ the distortion function appropriate to that distance. Actually, it is sufficient if the distortion is calibrated for two distinct focal settings, for then the distortion for any other setting can be computed from theory. Thus, even though the distortion function may be known from a stellar calibration, the problem remains of calibrating distortion for at least one, and preferably two (the second to serve as a check), well spaced, finite focal settings.

In elaborating on this matter, we shall present developments which have been successfully employed at DBA Systems for almost a decade, but which, for proprietary reasons, have not hitherto been disclosed.

ABSTRACT: *For highest accuracies it is necessary in close range photogrammetry to account for the variation of lens distortion within the photographic field. A theory to accomplish this is developed along with a practical method for calibrating radial and decentering distortion of close-range cameras. This method, the analytical plumb line method, is applied in an experimental investigation leading to confirmation of the validity of the theoretical development accounting for variation of distortion with object distance.*

EXTENSION OF MAGILL'S MODEL

Magill (1955) derived and experimentally verified a formula which accounts for the variation of distortion with changing focus. Magill's result can be expressed as follows. Let:

f = focal length of lens,
s = distance of object plane for which lens is focussed,
δr_s = distortion function for focus on object plane at distance s,
δr_∞ = distortion function of lens for infinity focus,
$\delta r_{-\infty}$ = distortion function of lens for inverted infinity focus (i.e., distortion, if the lens is reversed so that front element becomes rear element and vice versa).

Then the magnification of the lens for the object plane at s is

$$m_s = f/(s - f) \qquad (1)$$

* Presented at the Symposium on Close-Range Photogrammetry, Urbana, Illinois, January 1971.

and Magill's formula states that

$$\delta r_s = \delta r_{-\infty} - m_s \delta r_{\infty}. \tag{2}$$

This formulation is convenient enough when distortion is determined on an optical bench with the aid of a collimator and goniometer (as in Magill's investigation), for then $\delta r_{-\infty}$ and δr_{∞} can be determined with equal facility. Otherwise, the determination of $\delta r_{-\infty}$ for a lens already mounted in a camera becomes physically so awkward as to be impractical in most instances. Accordingly, as it stands, Magill's formula is of rather limited practical value. However, a more convenient result can be derived from the formula by the following process. Let s_1 and s_2 denote two arbitrary distances of object planes for which the distortion functions δr_{s_1}, δr_{s_2} are known. If s_1 and s_2 are substituted into Equation 2, the resulting pair of equations can be solved for $\delta r_{-\infty}$ and δr_{∞} as functions of δr_{s_1} and δr_{s_2}. If these solutions are then employed in Equation 2 one obtains

$$\delta r_s = \alpha_s \delta r_{s_1} + (1 - \alpha_s)\delta r_{s_2} \tag{3}$$

where

$$\alpha_s = \frac{s_2 - s}{s_2 - s_1}\,\frac{s_1 - f}{s - f}. \tag{4}$$

Accordingly, it follows that if the distortion functions δr_{s_1}, δr_{s_2} are known for the lens focussed on any two distinct object planes, the distortion function δr_s for the lens focussed on any other plane can be computed by means of Equation 3. This extension of Magill's formula is well suited to general application.

If δr_{s_1} and δr_{s_2} are expressed in the usual representation as power series in radial distance r, so that

$$\begin{aligned} \delta r_{s_1} &= K_{1s_1} r^3 + K_{2s_1} r^5 + K_{3s_1} r^7 + \cdots \\ \delta r_{s_2} &= K_{1s_2} r^3 + K_{2s_2} r^5 + K_{3s_2} r^7 + \cdots \end{aligned} \tag{5}$$

one obtains from Equation 3 the result that the coefficients in the expansion

$$\delta r_s = K_{1s} r^3 + K_{2s} r^5 + K_{3s} r^7 + \cdots \tag{6}$$

are given by

$$\begin{aligned} K_{1s} &= \alpha_s K_{1s_1} + (1 - \alpha_s) K_{1s_2} \\ K_{2s} &= \alpha_s K_{2s_1} + (1 - \alpha_s) K_{2s_2} \\ K_{3s} &= \alpha_s K_{3s_1} + (1 - \alpha_s) K_{3s_2}. \end{aligned} \tag{7}$$

Certain special cases of Equation 3 merit consideration. If, as would often be the case, one of the known distortion functions corresponds to focus at infinity (i.e., $s_2 = \infty$), the formula for α_s reduces to

$$\alpha_s = (s_1 - f)/(s - f). \tag{8}$$

If, in addition, the second known distortion function corresponds to unit magnification (i.e., $s_1 = 2f$), α_s becomes

$$\alpha_s = f/(s - f) = m_s \tag{9}$$

where, as indicated in Equation 1, m_s is the magnification of the image for object plane at distance s. It is well known that for perfectly symmetric lenses, distortion at unit magnification is zero (i.e., $\delta r_{2f} = 0$), in which case, Equation 3 in conjunction with 9 assumes the specialized form

$$\delta r_s = (1 - m_s)\delta r_{\infty}. \tag{10}$$

This result is more of theoretical than practical interest, because most modern lenses that are classified as symmetric do, in fact, depart somewhat from perfect symmetry in their design.

Unless the lens designer is specifically concerned with the reduction of distortion to very low levels (as with aerial mapping lenses), it is likely that the distortion function over the usable field will be totally dominated by $K_1 r^3$, the leading term of the power series expansion (higher order terms $K_2 r^5, K_3 r^7$ only rarely assume significance in commercial lenses not specifically designed for photogrammetric applications). When higher order terms are insignificant for a given lens, Equation 3 has a consequence of special importance to some applications; it implies the existence of an object plane distance for which distortion is zero. If we set $s_1 = 2f$, $s_2 = \infty$ in Equation 3 and then equate δr_s to zero, we shall obtain a linear equation in s, the solution of which is

$$s = \left(2 - \frac{\delta r_{2f}}{\delta r_{\infty}}\right) f = \left(2 - \frac{K_{1,2f}}{K_{1\infty}}\right) f. \tag{11}$$

This defines the object plane distance for which the distortion of the lens will be zero throughout the field (or, more precisely, for which the leading coefficient K_{1s} will be zero). If δr_{2f} and δr_{∞} are initially unknown, they can, of course, be computed from Equation 3, provided δr_{s_1} and δr_{s_2} are known. Equation 11 can be helpful in selection of a lens for a project where low distortion is desirable for the magnification to be employed.

Variation of Distortion Throughout the Photographic Field

Magill's formula accounts only for distortion of points within the particular object plane for which the lens is focussed. It does not precisely account for distortion for other, less sharply focussed points within the photographic field. To clarify this matter, let us consider the specific case of a lens that has

been focussed for an object plane 4 feet away. If the lens has a focal length of about 5 inches and is stopped down to $f/45$, the useful field may range between a near field of about 3 feet and a far field of 6 feet. One could, of course, validly employ Magill's formula to compute the distortion for $s=4$ feet. However, as we shall see, one could not validly proceed to employ Magill's formula to account for the distortion for points at $s=3$ feet or $s=6$ feet as long as the camera is actually focussed at 4 feet. This could, in fact, lead to an appreciable error. What is needed, then, is a further extension of Magill's formula to account for the variation of distortion for points distributed throughout the photographic field. Anticipating such a development, we shall introduce the notation $\delta r_{s,s'}$ to denote the distortion function corresponding to points in an object plane at distance s' for a lens that is focussed on an object plane at distance s.

The relationship we seek can be readily derived with the aid of Figure 1 which is largely self explanatory. From similar triangles we have the relations

$$r' = \gamma_{s,s'} r \tag{12}$$

$$\delta r_{s,s'} = \frac{1}{\gamma_{s,s'}} \delta r_{s'} \tag{13}$$

where

$$\gamma_{s,s'} = c_{s'}/c_s. \tag{14}$$

We may express $\delta r_{s'}$ as

$$\delta r_{s'} = K_{1s'}(r')^3 + K_{2s'}(r')^5 + K_{3s'}(r')^5 + \cdots \tag{15}$$

Replacing r' by $\gamma_{s,s'} r$ in Equation 15 and substituting the result into 13, we get

$$\delta r_{s,s'} = \overset{2}{\gamma}_{s,s'} K_{1s'} r^3 + \overset{4}{\gamma}_{s,s'} K_{2s'} r^5 + \overset{6}{\gamma}_{s,s'} K_{3s'} r^7 + \cdots \tag{16}$$

the desired result. According to the thin lens law

$$\frac{1}{s} + \frac{1}{c_s} = \frac{1}{f}$$
$$\frac{1}{s'} + \frac{1}{c_{s'}} = \frac{1}{f}. \tag{17}$$

From these relations and Equations 1 and 14 follow the alternative expressions for $\gamma_{s,s'}$,

$$\gamma_{s,s'} = \frac{s-f}{s'-f}\frac{s'}{s} = \frac{s' m_{s'}}{s m_s}. \tag{18}$$

We are now in a position to outline the steps involved in the process of correcting for distortion of points distributed throughout the photographic field. We assume first that distortion functions $\delta r_{s_1}, \delta r_{s_2}$ have been previously

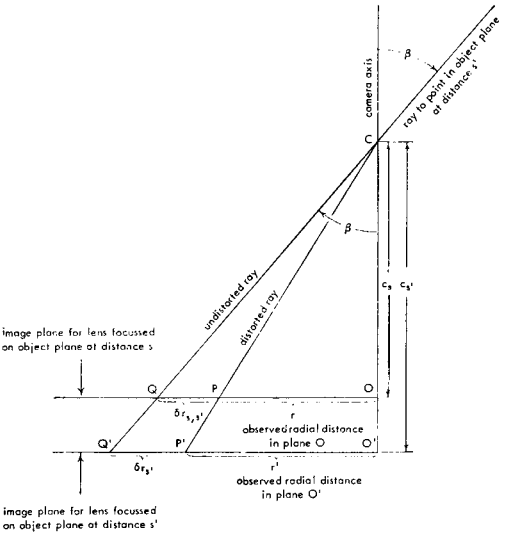

FIG. 1. Illustrating the geometric relationship between $\delta r_{s'}$, and $\delta r_{s,s'}$.

calibrated (later we shall concern ourselves with how this is to be done). Then the steps of the corrective process are as follows:

a. approximate coordinates X, Y, Z of the photographed point are determined by photogrammetric triangulation using plate coordinates that are either uncorrected for distortion or are corrected for the distortion corresponding to the object plane at distance s on which the lens is focussed; this permits the distance s' to the object plane containing X, Y, Z to be computed;

b. with s' known, Equation 4 is evaluated to obtain $\alpha_{s'}$ which is then substituted into 7 to generate the coefficients $K_{1s'}$, $K_{2s'}$, $K_{3s'}$;

c. $\gamma_{s,s'}$ is then evaluated by means of Equation 14 or 18 which together with the coefficients $K_{1s'}$, $K_{2s'}$, $K_{3s'}$ permits the distortion function 16 to be evaluated for the observed radial distance r of the image;

d. with $\delta r_{s,s'}$ thus evaluated, the corrections to be added to the measured plate coordinates x, y (referred to the principal point as origin) are computed from the usual formulas: $\delta x = (x/r)\delta r_{s,s'}$, $\delta y = (y/r)\delta r_{s,s'}$;

e. the corrected plate coordinates for each camera are employed to effect a revised triangulation, generating improved X, Y, Z coordinates which may, if deemed desirable, be employed in an iteration of the above process.

Later in this paper we shall present experimental verification of the above development.

METHODS OF CAMERA CALIBRATION DEVELOPED BY DBA

The general analytical calibration of cameras focussed at infinity was originally developed in Brown (1956). Extensions of this theory to account for errors in control points and for effects of lens decentering were pub-

lished in Brown (1964) and in Brown (1965). A further generalization to permit determination of distortion by means of the simultaneous reduction of measurements from an unlimited number of frames taken by a given camera is embodied in the SMAC (Simultaneous Multiframe Analytical Calibration) reduction published in Brown (1968). All previous developments had been concerned with extraction of distortion from measurements of a single frame or plate having the essential property of invariant orientation throughout the total exposure. In application to stellar calibrations, SMAC made it possible to do away with the conventional requirement that the orientation of the camera remain perfectly stable for all exposures on a given plate; it also did away with the conventional requirement that the times of the stellar exposures be accurately known. In application to aerial calibration, SMAC provided the rigorous solution to the problem of deriving a definitive calibration from the merging of an indefinitely large number of frames exposed over an aerial calibration range.

As far as applications to close-range photography are concerned, the methods cited above have served mainly to calibrate δr_∞, thus providing one of the two distortion functions needed in our extension of Magill's formula. In principle, Aerial SMAC could be employed to reduce exposures of a carefully constructed and very accurately surveyed calibration range specifically designed for close-range photogrammetry. This would provide the second of the two needed distortion functions. We, however, have not chosen to adopt this approach, largely because of practical problems associated with constructing and maintaining a suitable target range, but also because of our development and implementation of two alternative methods which have proven extremely effective.

The first of these two methods is a process of self-calibration effected by incorporating our extension of Magill's formula into the process of multistation analytical stereotriangulation that was originally developed in Brown (1958). Our computer program for structural measurements can accommodate observations from up to nine exposure stations. It requires that distortion coefficients be precalibrated for one object plane s_2 (usually, $s_2 = \infty$) and regards as unknown the distortion coefficients for the particular object plane on which the camera is focussed. It also regards coefficients of decentering distortion as being unknown. The reduction requires no absolute control points (but can exercise them, if available) and can accommodate an indefinitely large number of passpoints. If highly convergent geometry from three or more exposure stations is exercised, the program can also accomplish an accurate calibration of the coordinates of the principal point x_p, y_p. If, in addition, at least one distance between targets in object space is known, the program can also recover the principal distance c of the camera (otherwise, a pre-established value of c must be enforced). We shall not go further into the method of self-calibration inasmuch as a separate paper on the method is in preparation.

In those photogrammetric projects in which the same camera can be used for all needed exposures, our policy has been to employ the method of self-calibration just described with the project itself providing the observational material needed for the calibration. Thus, in such endeavors we do not find it necessary to pre-calibrate the camera for the project. However, in some projects a different camera must be employed at each of the exposure stations. Such projects include mensuration of nonstatic structures and mensuration of structures inside environmental test chambers. Here, self-calibration is ineffective because each exposure station requires recovery of a fresh set of distortion coefficients. This brings us to the second of the two special methods of camera calibration that we have employed in conjunction with close-range photogrammetry. It is one particularly well suited to the task of pre-calibrating a camera for a specified focal setting. As was pointed out in our original paper on photogrammetric structural measurements (Brown (1962)), this method "involves photographing a set of plumb lines arrayed in the desired object plane and exploits the fact that, in the absence of distortion, the central projection of a straight line is itself a straight line. Systematic deviations of the images of plumb lines from straight lines thus provide a measure of distortion if properly reduced."

Because details of the analytical plumb-line method, as we shall call it (to distinguish it from older, more qualitative plumb-line approaches such as that described by Cox (1956)), have not hitherto been published, we shall outline the essentials of the method here. As is clear from Figure 2, the equation of an arbitrary straight line L on a plate can be expressed as

$$x' \sin\theta + y' \cos\theta = \rho \qquad (19)$$

where ρ denotes distance of the line from the origin and θ is the angle between the y'-axis

and the normal to the line passing through the origin. Because of radial and decentering distortion the image of a photographed plumb line will not be truly straight. However, if the coordinates x, y of points on the image of a plumb line were corrected for such distortion, they would conform to a straight line. According to Brown (1964), (1965), coordinates so corrected can be expressed as

$$\begin{aligned} x' &= x+\bar{x}(K_1r^2+K_2r^4+K_3r^6+\cdots) \\ &\quad +[P_1(r^2+2\bar{x}^2)+2P_2\bar{x}\bar{y}][1+P_3r^2+\cdots] \\ y' &= y+\bar{y}(K_1r^2+K_2r^4+K_3r^6+\cdots) \\ &\quad +[2P_1\bar{x}\bar{y}+P_2(r^2+2\bar{y}^2)][1+P_3r^2+\cdots] \end{aligned} \tag{20}$$

in which

$$\begin{aligned} \bar{x} &= x - x_p \\ \bar{y} &= y - y_p \\ r &= [(x - x_p)^2 + (y - y_p)^2]^{1/2} \end{aligned} \tag{21}$$

and K_1,K_2,K_3 are coefficients of radial distortion (for the object plane being observed) and P_1,P_2,P_3 are coefficients of decentering distortion. Let us now consider images of a set of plumb lines on a given plate and let x_{ij},y_{ij} denote the plate coordinates of the jth measured point on the i-th line. If we then substitute x_{ij},y_{ij} into Equations 20 and 21 and substitute the resulting expressions into 19 we shall obtain an observational equation that is functionally of the form

$$f(x_{ij}, y_{ij}; x_p, y_p, K_1, K_2, K_3, P_1, P_2, P_3; \theta_i, \rho_i) = 0. \tag{22}$$

If m denotes the total number of lines measured and n_i denotes the number of points measured on the i-th line, the total number of equations of the form 22 will amount to

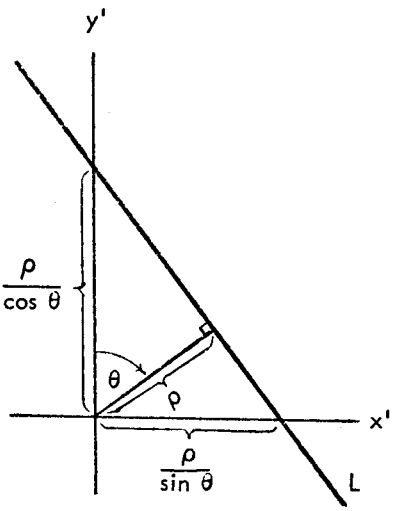

FIG. 2. Explanation of the plumb-line method.

$$n = n_1 + n_2 + \cdots + n_m. \tag{23}$$

This set of equations will involve a total of $8+2m$ parameters consisting of the eight parameters of the inner cone $x_p,y_p,K_1,K_2,K_3,P_1,P_2,P_3$ (which are common to all lines) and a pair of parameters θ_i,ρ_i for each of the m lines. It follows that if a sufficient number of points are measured on each line, the number of equations will exceed the number of unknowns and a least-squares adjustment is in order.

To effect such an adjustment we first set

$$\begin{aligned} x_{ij} &= x_{ij}{}^0 + v_{x_{ij}} \\ y_{ij} &= y_{ij}{}^0 + v_{y_{ij}} \end{aligned} \tag{24}$$

where $x_{ij}{}^0,y_{ij}{}^0$ are the actually measured coordinates and the v's are corresponding residuals. For the parameters we then set

$$\begin{aligned} x_p &= x_p{}^{00} + \delta x_p \\ y_p &= y_p{}^{00} + \delta y_p \\ &\vdots \\ \rho_1 &= \rho_i{}^{00} + \delta\rho_i \end{aligned} \tag{25}$$

where the superscripts $(^{00})$ denote known approximations and the δ's are unknown corrections. By substituting Equations 24 and 25 into 22 and then linearizing the resulting expression by Taylor's expansion, we obtain the following set of observational equations:

$$\underset{(1,\,2)(2,\,1)}{A_{ij}}\ \underset{}{v_{ij}} + \underset{(1,\,8)(8,\,1)}{\dot{B}_{ij}}\ \underset{}{\dot{\delta}} + \underset{(1,\,2)(2,\,1)}{\ddot{B}_{ij}}\ \underset{(1,\,1)}{\ddot{\delta}_1} = \epsilon_{ij}, \qquad \begin{matrix} i = 1, 2, \cdots, m \\ j = 1, 2, \cdots, n_i \end{matrix} \tag{26}$$

in which

$$\epsilon_{ij} = -f(x_{ij}{}^0, y_{ij}{}^0; x_p{}^{00}, y_p{}^{00}, K_1{}^{00}, \cdots, P_3{}^{00}, \theta_i{}^{00}, \rho_i{}^{00}) \tag{27}$$

$$v_{ij} = \begin{bmatrix} v_{x_{ij}} \\ v_{y_{ij}} \end{bmatrix}, \quad \delta = \begin{bmatrix} \delta x_p \\ \delta y_p \\ \delta K_1 \\ \vdots \\ \delta P_3 \end{bmatrix}, \quad \ddot{\delta}_i = \begin{bmatrix} \delta\theta_i \\ \delta\rho_i \end{bmatrix} \tag{28}$$

and the coefficient matrices $A_{ij},\dot{B}_{ij},\ddot{B}_{ij}$ are the Jacobians

$$\begin{aligned} A_{ij} &= -\frac{\partial\epsilon_{ij}}{\partial(x_{ij}{}^0, y_{ij}{}^0)} \\ \dot{B}_{ij} &= -\frac{\partial\epsilon_{ij}}{\partial(x_p{}^{00}, y_p{}^{00}, K_1{}^{00}, \cdots, P_3{}^{00})} \\ \ddot{B}_{ij} &= -\frac{\partial\epsilon_{ij}}{\partial(\theta_i, \rho_i)}. \end{aligned} \tag{29}$$

If we initially confine ourselves to consideration of the set of normal equations generated by the observations of the i-th line, we

shall obtain the following result upon applying the generalized least-squares theory developed in Brown (1955):

$$\begin{bmatrix} \dot{N}_i & \overline{N}_i \\ (8,8) & (8,2) \\ \overline{N}_i^T & \ddot{N}_i \\ (2,8) & (2,2) \end{bmatrix} \begin{bmatrix} \dot{\delta} \\ (8,1) \\ \ddot{\delta}_i \\ (2,1) \end{bmatrix} = \begin{bmatrix} \dot{c}_i \\ (8,1) \\ \ddot{c}_i \\ (2,1) \end{bmatrix} \tag{30}$$

where

$$\begin{aligned} \dot{N}_i &= \sum \dot{N}_{ij}, \quad \dot{c}_i = \sum \dot{c}_{ij}, \\ \overline{N}_i &= \sum \overline{N}_{ij}, \quad \ddot{c}_i = \sum \ddot{c}_{ij}, \\ \ddot{N}_i &= \sum \ddot{N}_{ij}, \end{aligned} \tag{31}$$

in which all summations range from $i=1$ to $i=n_i$, and in which

$$\begin{aligned} \dot{N}_{ij} &= p_{ij}\dot{B}_{ij}{}^T\dot{B}_{ij}, \quad \dot{c}_{ij} = p_{ij}\dot{B}_{ij}{}^T\epsilon_{ij} \\ \overline{N}_{ij} &= p_{ij}\dot{B}_{ij}{}^T\ddot{B}_{ij}, \quad \ddot{c}_{ij} = p_{ij}\ddot{B}_{ij}{}^T\epsilon_{ij} \\ \ddot{N}_{ij} &= p_{ij}\ddot{B}_{ij}{}^T\ddot{B}_{ij}. \end{aligned} \tag{32}$$

In Equations 32, p_{ij} is the scalar

$$\begin{matrix} p_{ij} & = & (& A_{ij} & \Lambda_{ij} & A_{ij}{}^T)^{-1} \\ (1,1) & & & (1,2) & (2,2) & (2,1) \end{matrix} \tag{33}$$

in which Λ_{ij} denotes the covariance matrix of $x_{ij}{}^0, y_{ij}{}^0$. In the derivation of the above result we made the usual assumption that plate coordinates of different points are uncorrelated.

Because observational vectors are independent from line to line, we may employ the *zero augmentation* merging process originally developed in Brown, Trotter (1967) to generate the system of normal equations resulting from the simultaneous adjustment to all observations from all lines. This system is of the form:

$$\left[\begin{array}{c|cccc} \dot{N}+\dot{W} & \overline{N}_1 & \overline{N}_2 & \cdots & \overline{N}_m \\ \hline \overline{N}_1{}^T & \ddot{N}_1 & 0 & \cdots & 0 \\ \overline{N}_2{}^T & 0 & \ddot{N}_2 & \cdots & 0 \\ \vdots & \vdots & \vdots & & \vdots \\ \overline{N}_m{}^T & 0 & 0 & \cdots & \ddot{N}_m \end{array}\right] \left[\begin{array}{c} \dot{\delta} \\ \hline \ddot{\delta}_1 \\ \ddot{\delta}_2 \\ \vdots \\ \ddot{\delta}_n \end{array}\right] = \left[\begin{array}{c} \dot{c}-\dot{W}\dot{\epsilon} \\ \hline \ddot{c}_1 \\ \ddot{c}_2 \\ \vdots \\ \ddot{c}_n \end{array}\right] \tag{34}$$

in which

$$\dot{N} = \sum_{i=1}^{m} \dot{N}_i, \quad \dot{c} = \sum_{i=1}^{m} \dot{c}_i. \tag{35}$$

The terms $\dot{W}$ and $\dot{W}\dot{\epsilon}$ account for any *a priori* values of the parameters in $\dot{\delta}$ that are to be exercised according to the development of Brown (1959) (specifically, $\dot{W}$ is the inverse of the parameters and $\dot{\epsilon}$ is the discrepancy vector between the *a priori* values themselves and the approximations being exercised in the current linearization).

The general system of normal Equations 34 is of the by-now-familiar form first investigated in Brown (1958) and further treated in Brown, Trotter (1969). The order of the normal equations is $2m+8$ and thus increases linearly with the number of lines being carried in the reduction. Ordinarily, this would set a practical limit of the number of lines that can be processed simultaneously. However, as is shown in Brown (1958) the block diagonality of the $\ddot{N}$ portion of the normal equations can be exploited to generate an algorithm for the practical solution of the system no matter how large m may become. The essential steps of the algorithm are as follows. In terms of the basic matrices generated in Equation 30 for the i-th line, the following auxiliaries are formed:

$$\begin{matrix} Q_i & = & \ddot{N}_i{}^{-1} & \overline{N}_i{}^T, & \\ (2,8) & & (2,2) & (2,8) & \\ R_i & = & \overline{N}_i & Q_i & \\ (8,8) & & (8,2) & (2,8) & \\ S_i & = & \dot{N}_i & - & R_i, \\ (8,8) & & (8,8) & (8,8) & \\ \bar{c}_i & & \dot{c}_i & Q_i{}^T & \ddot{c}_i \\ (8,1) & & (8,1) & (8,2) & (2,1) \end{matrix} \tag{36}$$

As S_i and $\bar{c}_i$ are formed, they are added to the sum of their predecessors and only cumulative result is retained. The end result of this process, once all m lines have been processed, is

$$\begin{aligned} S &= S_1 + S_2 + \cdots + S_m, \\ \bar{c} &= \bar{c}_1 + \bar{c}_2 + \cdots + \bar{c}_m. \end{aligned} \tag{37}$$

The solution for the vector $\dot{\delta}$ is then given by

$$\dot{\delta} = (S + \dot{W})^{-1}(\bar{c} - \dot{W}\dot{\epsilon}). \tag{38}$$

After $\dot{\delta}$ has been obtained, the vector of parameters $\ddot{\delta}_i$ for each line is computed from

$$\ddot{\delta}_i = \ddot{N}_i{}^{-1}\ddot{c}_i + Q_i\dot{\delta}_i, \qquad (i = 1, 2, \cdots, m). \tag{39}$$

It will be noted that the largest matrix to be generated, inverted or otherwise operated on in the above process is only of order 8×8. Moreover, the computational effort increases only linearly with the number of lines to be reduced. Hence there is no limit to the number of lines that can be processed simultaneously.

The covariance matrix of the adjusted parameters in $\dot{\delta}$ is given by the term $(S+\dot{W})^{-1}$ in Equation 38. From this one can

compute error bounds to be associated with the calibrated distortion functions.

If the adjustment is iterated to convergence, the final plate measuring residuals can be computed from

$$\underset{(2,\,1)}{v_{ij}} = \begin{bmatrix} v_{x_{ij}} \\ v_{y_{ij}} \end{bmatrix} = \underset{(2,\,2)}{p_{ij}} \underset{(2,\,1)}{\Lambda_{ij}} \underset{(1,\,1)}{A_{ij}^T} \epsilon_{ij} \qquad (40)$$

in which ϵ_{ij} denotes the value computed from the final values of the parameters. The mean error of the residuals is given by

$$s = \left[\sum_{i=1}^{n} \sum_{j=1}^{n_i} v_{ij}^T \Lambda_{ij}^{-1} v_{ij} / \text{d.o.f.} \right]^{1/2} \qquad (41)$$

in which the degrees of freedom (*d.o.f.*) are given by

$$\text{d.o.f.} = n - p - 2m \qquad (42)$$

in which p denotes the number of projective parameters being exercised.

The observational equations for the analytical plumb line method do not involve exterior elements of orientation ($\alpha,\omega,\kappa,X^c,Y^c,Z^c$) nor do they involve the principal distance c. As a result, one is free to employ multiple exposures of one or more plumb lines to generate as many images as desired as long as all correspond to a common plane in the object space. The most attractive feature of the plumb line method is its observational simplicity. By contrast, the preparation of a special target range of accuracy and stability sufficient for close range calibration is a formidable and expensive undertaking. In the next section we shall review specific applications of the analytical plumb line method.

Experimental Verification of Theoretical Findings

In this section we shall present results of a series of calibrations that serve to:

- Demonstrate the efficacy of the analytical plumb line method of calibration;
- Provide a check on the validity of Equation 3 in accounting for change of distortion with change of focus;
- Provide a check on the validity of Equation 16 in accounting for change of distortion within the photographic field.

The lens employed in the calibrations is a standard commercial Schneider Symmar of 135mm focal length. The lens, mounted in a threaded barrel, was installed in one of DBA's structural measurement cameras (Figure 3) having a circular format six inches in diameter (with the 135 mm lens, this corresponds to a cone angle of about 60°). On actual projects of structural measurements, focussing of

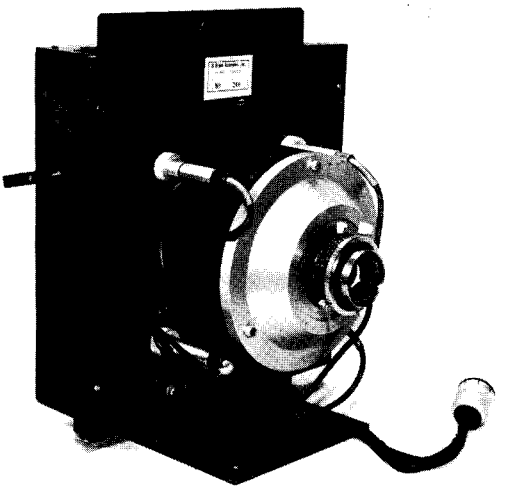

FIG. 3. Single-frame glass-plate camera fabricated by DBA for close-range structural measurements. The camera accepts 190×215 mm×$\frac{1}{4}$ inch ballistic plates and exposes a 6-inch diameter format. Interchangeable cones allow focussing from 2 feet to infinity.

the camera is accomplished by means of precise, dowelled spacers mounted between the lens plate and the camera body. This permits x_p,y_p and c to be related to the values obtained from a stellar calibration to a precision of about 10 micrometers. For the plumb line exercises, however, we considered the fabrication of special spacers to be unwarranted and, instead, focussed the lens by screwing the threaded mounting barrel from its standard setting for infinity focus.

To test our theoretical findings, we decided to perform a series of five plumb line calibrations with relative aperture set at $f/45$ to insure a fairly deep field of acceptable focus. The five calibrations correspond to the situations indicated in Table 1. For each case, an array of seven plumb lines was set up in the indicated plane with line-to-line spacing adjusted between exposures to maintain a spacing of nominally 20mm between images of the plumb lines on the photographic plate. The plumb lines were made of very fine white thread and were stabilized by immersion of the plumb bobs in containers of oil. Illumination was provided by a pair of vertically mounted, 8-foot fluorescent fixtures that could be freely positioned for optimum distribution of light. A dead black background was provided for the plumb-line array in order to heighten contrast and to permit the execution of multiple exposures on the same plate. For each of the indicated cases two exposures were

TABLE 1. CASES CONSIDERED IN EXPERIMENTAL INVESTIGATIONS BASED ON ANALYTICAL PLUMB LINE METHOD OF CAMERA CALIBRATION

Case	*Camera focus set for object plane at distance s (ft)*	*Plumb lines in common plane at distance s' (ft)*
1	3	3 (mid field)
2	4	3 (near field)
3	4	4 (mid field)
4	4	6 (far field)
5	6	6 (mid field)

made on a given plate with the camera rolled nominally 90° between exposures. A reproduction of one of the plates is provided by Figure 4. All five plates are essentially alike in appearance by virtue of the adjustment of plumb line spacing from one case to the next. Focussing on each of the indicated object planes was accomplished visually at full aperture ($f/5.6$) by observing on ground glass the magnified image of a rear-illuminated bar target at the center of the object plane.

On each of the five plates, points on the lines were measured at 5mm intervals on DBA's digitzed Mann comparator. This generated a total of 324 points per plate (162 from the horizontal lines and 162 from the vertical lines). The measuring process required from 5 to 6 hours per plate. Each set of observations was processed through the analytical plumb-line program on DBA's Xerox Sigma 5 computer. Typical total job time per plate was just under four minutes. Key results of the reductions are presented in Table 2. Also listed in the table as Case 6 are results of a stellar SMAC calibration that had been performed two years earlier on the same lens. The stellar calibration employed a total of 302 measured stellar images, a number comparable to the number of points measured on the plumb line plates.

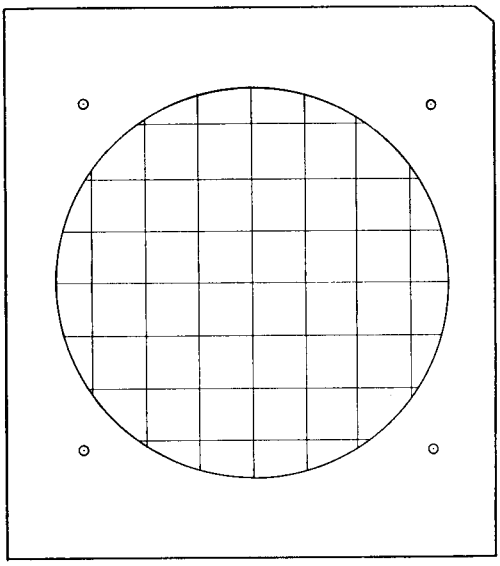

FIG. 4. Appearance of typical plate employed in plumb-line calibrations.

From the table we note that the *rms* values of the residuals obtained from the analytical plumb line calibration are all appreciably lower than that obtained from the stellar calibration. This suggests that settings can be made on arbitrary points on well defined lines to significantly greater accuracy than they can on point-like images. Only the leading coefficient K_1 of the radial distortion function was found to contribute to the adjustment. Results for decentering distortion are

TABLE 2. SUMMARY OF KEY RESULTS OF CALIBRATIONS

Case	*s*	*s'*	*RMS value of residuals*	*Radical distortion*		*Decentering distortion*			
			m (μm)	$10^6 K_1$ $(mm)^{-2}$	$10^6 \sigma_{K_1}$ $(mm)^{-2}$	$10^5 J_1$ $(mm)^{-1}$	$10^5 \sigma_{J_1}$ $(mm)^{-1}$	φ (*deg*)	σ_φ (*deg*)
1	3	3	1.6	− .628	.0023	.292	.010	61.7	1.9
2	4	3	1.6	− .699	.0023	.345	.009	50.6	1.9
3	4	4	1.4	− .719	.0017	.338	.007	47.6	1.7
4	4	6	1.8	− .740	.0025	.320	.011	53.4	2.1
5	6	6	1.8	− .825	.0023	.324	.001	43.4	2.1
6	∞	∞	2.7	−1.024	.0028	.397	.013	37.5	2.0

Note: All values of φ have been corrected for rotation of lens barrel in order to facilitate direct intercomparison with infinity calibration (Case 6).

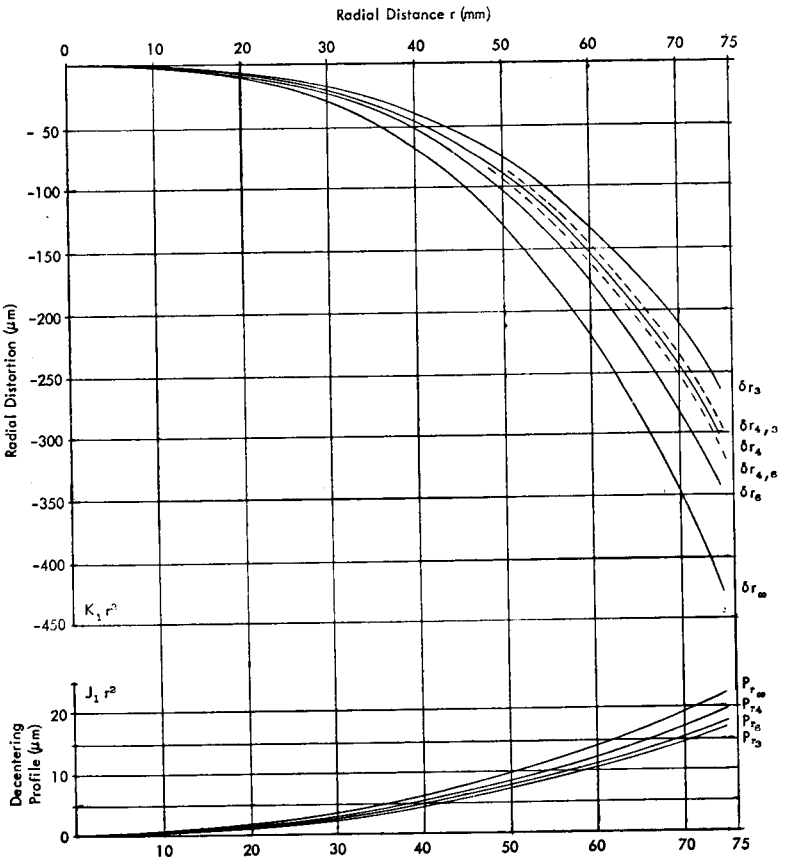

FIG. 5. Plots of radial distortion functions (upper) and decentering profile functions (lower) given in Table 3 (profile functions $Pr_{4,3}$ and $Pr_{4,6}$ nearly coincide with Pr_4 and Pr_6, respectively, and hence are not plotted).

expressed in terms of the profile parameter defined by

$$J_1 = \sqrt{(P_1^2 + P_2^2)}$$

and phase angle φ of the axis of maximum tangenital distortion given by the relationship

$$\tan \vartheta = -P_1/P_2.$$

Graphical representations of the radial distortion function K_1r^3 and the decentering profile function J_1r^2 are provided in Figure 5 for each of the six cases in Table 2. Standard deviations of the plotted curves, though not plotted, generally do not exceed one micrometer at the maximum radial distance of 75 mm.

Figure 5 shows clearly the systematic nature of the variation of radial and decentering distortion with object distance. The radial distortion for the Symmar lens, it will be noted, is rather large, growing at infinity focus to 430 μm for $r = 75$ mm. This is precisely why we selected the Symmar for the investigation; the laws governing variation of distortion with object distance would clearly be much more difficult to verify experimentally with a lens of low distortion. Results listed in Table 2 are employed in Tables 3 and 4 to compute the distortion functions δr_4, $\delta r_{4,3}$, $\delta r_{4,6}$ from the calibrated distortion functions δr_3, δr_6. Agreement between observed and computed values is very good, being generally better than two percent. In computing the values $\gamma_{s,s'}$ to be used in Equation 16, we employed the relation $\gamma_{s,s'} = c_s/c_{s'}$ given by Equation 14 rather than the alternate relation given by 18. This is because precise values of c were available by direct measurement (from the number of turns of the focussing barrel). These values in inches are

$$c_3 = 6.222$$
$$c_4 = 5.950$$
$$c_6 = 5.692$$

TABLE 3. COMPARISON OF CALIBRATED DISTORTION FOR $s=4$ FEET WITH RESULTS COMPUTED FROM EQUATION 3 USING CALIBRATED DISTORTION FUNCTIONS FOR $s_1=3$ FEET AND $s_2=6$ FEET.

r (mm)	δr_4 *Observed* (μm) $-.719\times10^6 r^3$	δr_4 *Computed* (μ,) $-.730\times10^6 r^3$	*Difference* O - C (μm)
15	− 2.4	− 2.5	0.1
30	− 19.4	− 19.7	0.3
45	− 65.5	− 66.5	1.0
60	−155.2	−157.8	2.6
75	−303.2	−308.0	4.8

Note: Because $f=5.300$ inches the value of α_4 in Equation 3 turns out to be equal to .480 for $s_1=3$ feet and $s_2=6$ feet.

which leads to the values

$$\gamma_{4,3} = .956$$
$$\gamma_{4,6} = 1.047.$$

Because of the inexactness of the focussing process, somewhat poorer values would have been obtained from the application of Equation 18. In retrospect, we now appreciate that the values of s employed for the experimental set up should have been computed from the measured values of c. The various expressions for $\gamma_{s,s'}$ would then have produced identical values. It seems quite possible that even better results might have been obtained in Tables 3 and 4 had this precaution been taken. As it is, the results are in good agreement with theoretical expectations.

Although we have yet to develop a specific theoretical model to account for the variation of decentering distortion with object distance, some observations on our experimental findings are in order. First we note in Figure 4 that a small systematic change in the profile function does accompany changes in focal setting (the spread of 6 μm between the profiles at $r=75$ mm for 3 feet and ∞ is too great to be accidental). On the other hand, the variation of decentering distortion within the photographic field appears to be too small to be of practical significance. As far as the phase angle of decentering is concerned, one would not expect to find any variation in φ with focus after due allowance has been made for the rotation of the lens. Table 2 shows this substantially to be the case. There is no significant variation at all in φ between Cases 2, 3, 4; here the orientation of the lens is unchanged for all three calibrations. For the other cases, the relative change in φ is small, but not small enough to be insignificant. We believe this to be attributable to a slight misalignment between the axis of the lens and the axis of the focussing barrel. The variation in tilt that would thus be introduced by the focussing operation could well compromise the recovery of φ to the small extent observed.

It will be recalled that the coordinates of the principal point x_p,y_p were carried as adjustable parameters in the derivation of the plumb-line method. Upon application of the reduction we found, however, that these parameters are inherently indeterminate if parameters for decentering distortion P_1,P_2 are also carried as adjustable parameters. Even if P_1,P_2 are suppressed, the recovery of x_p,y_p is very weak, being accurate only to about 200 μm (one sigma) in the particular reductions considered above. Indeed the recoverability of x_p,y_p in the plumb-line calibration depends directly on the magnitude of the radial distortion; the greater the distortion, the better the recovery of x_p,y_p. Because of such considerations, we assigned an *a priori* sigma of 100 μm to x_p, y_p in all of the plumb line adjustments reported in Table 2. Despite this allowable degree of variation in x_p,y_p, the amount of adjustment in x_p,y_p was less than 1 μm in all cases. This indicates that any actual variation in x_p,y_p was, in fact, being projectively absorbed by the values of P_1 and P_2 resulting from the adjustment.

TABLE 4. COMPARISON OF CALIBRATED DISTORTION FUNCTIONS $\delta r_{s,s}$ FOR $s=4$ FEET, $s'=3$ FEET AND FOR $s=4$ FEET, $s'=6$ FEET WITH RESULTS COMPUTED FROM EQUATION 16 USING CALIBRATED DISTORTION FUNCTIONS FOR $s_1=3$ FEET AND $s'=6$ FEET

r (mm)	$\delta r_{4,3}$ *Observed* (μm) $-.699\times10^6 r^3$	$\delta r_{4,3}$ *Computed* (μm) $-.689\times10^6$	*Difference* O-C (μm)	$\delta r_{4,6}$ *Observed* (μm) $-.740\times10^6 r^3$	$\delta r_{4,6}$ *Computed* (μm) $-.753\times10^6 r^3$	*Difference* O-C (μm)
15	− 2.4	− 2.3	−0.1	− 2.5	− 2.5	0.0
30	− 18.9	− 18.6	−0.3	− 20.0	− 20.3	0.3
45	− 63.7	− 62.8	−0.9	− 67.4	− 68.7	1.3
60	−150.9	−148.8	−2.1	−159.7	−162.6	2.9
75	−294.7	−290.7	−4.0	−312.0	−317.8	5.8

General Considerations

In some practical situations the variation in distortion between the near and far photographic fields can amount to as much as 10 percent of the distortion at midfield. One might use this as an argument for selecting a lens of low distortion for close-range applications. Thus, if maximum distortion were only 10 μm, a 10 percent variation in distortion would not exceed a negligible 1.0 μm. However, one must be careful in such an assessment to use the Gaussian distortion function and not the equivalent distortion function that camera makers prefer to advertise. With the latter, the principal distance is adjusted to transform the Gaussian distortion function $(K_1r^3+K_2r^5+\cdots)$ into a projectively equivalent form $(K_0'r+K_1'r^3+K_2'r^5+\cdots)$ which passes through zero at some arbitrarily specified radial distance.

Although the equivalent distortion function for a given lens may indeed reach an advertised maximum of, say, only 10 μm, it should be appreciated that the corresponding Gaussian distortion function could well have a maximum 10 times larger. If so, a 10 percent variation in distortion between near and far fields would actually amount to as much as 10 μm rather than the 1.0 μm alluded to above. Our experience has shown that there is really no compelling reason to require that specially designed lenses of low distortion be employed in close-range photogrammetry. The fact is that almost any well regarded commercial lens can produce first-class results if radial and decentering distortion are properly taken into account. As evidence of this, we would cite our experience in analytical triangulations performed with the 135 mm Symmar lens employed in calibrations considered above. Here, we have consistently obtained *rms* closures in plate coordinates of under 2.5 μm. Yet, this lens costs about $100 and is affected by a pronounced degree of radial and decentering distortion.

Strangely enough, lenses that are inferior by certain normal standards can be better suited to certain tasks than much more expensive, very highly corrected lenses. In close-range observations of parabolic antennas, for example, we have found that a lens having a curved field conforming approximately to the surface being measured is to be preferred over a lens with a flat field. Of course, curvature of field can be contrary to that of the subject, in which case it is detrimental. Thus, a lens having curvature of field well-suited to observations of parabolic reflectors would be ill-suited to external observations of a spherical surface and vice versa. One significant consequence of our findings is that the spectrum of lenses suitable for metric applications is so broadened that one has many relatively inexpensive alternatives to choose from in matching lenses with projects.

Conclusions

The analytical plumb-line method of calibrating radial and decentering distortion excells in operational convenience and is capable of producing results fully as accurate as those obtainable from extensive stellar calibrations. The application of the method to a series of close-range calibrations has served to support the theoretical development shown in a foregoing section by virtue of which one can account for the variation of distortion with focal setting and with object distance.

References

Brown, D. C., 1955. A Matrix Treatment of the General Problem of Least Squares Considering Correlated Observations. *Ballistic Research Laboratories Report No. 937.*

Brown, D. C. 1956. The Simultaneous Determination of the Orientation and Lens Distortion of a Photogrammetric Camera. *Air Force Missile Test Center Report No. 56-20,* Patrick AFB, Florida.

Brown, D. C., 1958. A Solution to the General Problem of Multiple Station Analytical Stereoangulation. *Air Force Missile Test Center Report No. 58-8,* Patrick AFB, Florida.

Brown, D. C., 1962. Precise Calibration of Surfaces of Large Radio Reflectors by Means of Analytical Photogrammetric Triangulation. *Research and Analysis Technical Report No. 10,* Instrument Corporation of Florida, Melbourne, Florida.

Brown, D. C., 1964. An Advanced Plate Reduction for Photogrammetric Cameras. *Air Force Cambridge Research Laboratories Report No. 64-40.*

Brown, D. C., 1965. Decentering Distortion of Lenses. Paper presented to the Annual Convention of the American Society of Photogrammetry, March 1965. Also published in *Photogrammetric Engineering* Vol. XXXII, No. 3. May 1966.

Brown, D. C., 1968. Advanced Methods for the Calibration of Metric Cameras. Final Report, Part 1, under Contract DA-44-009-AMC-1457 (X) to U.S. Army Engineering Topographic Laboratories, Fort Belvoir, Va. Also presented as paper to 1969 Symposium on Computational Photogrammetry sponsored by the American Society of Photogrammetry.

Brown, D. C., Trotter, J. E., 1969. Precise Determination of Geodetic Positions by the Method of Continuous traces. *Air Force Cambridge Research Laboratories Report No. 67-0558.*

Brown, D. C., Trotter, J. E., 1969. SAGA, A Computer Program for Short Arc Geodetic Adjustment of Satellite Observations. *Air Force*

Cambridge Research Laboratories Report No. 69-0080.

Cox, A., 1956. *Optics, the Technique of Definition.* Eleventh edition, The Focal Press, London and New York, page 255.

Kenefick, J. F., 1971. Ultra-Precise Analytical Stereotriangulation for Structural Measurements. Paper presented to the 1971 Symposium on Close-Range Photogrammetry sponsored by the American Society of Photogrammetry and conducted by the University of Illinois, Urbana, Illinois, January 26–29. 1971.

Magill, A. A., 1954. Variation in Distortion with Magnification. *Journal of Research of the National Bureau of Standards*, Vol. 54, No. 3, March 1955, pp. 135–142, Research Paper 2574.

Notice to Contributors

1. Manuscripts should be typed, double-spaced on $8\frac{1}{2}\times11$ or $8\times10\frac{1}{2}$ white bond, on *one* side only. References, footnotes, captions—everything should be double-spaced. Margins should be $1\frac{1}{2}$ inches.
2. *Two* copies (the original and first carbon) of the complete manuscript and two sets of illustrations should be submitted. The second set of illustrations need not be prime quality.
3. Each article should include an abstract, which is a *digest* of the article. An abstract should be 100 to 150 words in length.
4. Tables should be designed to fit into a width no more than five inches.
5. Illustrations should not be more than twice the final print size: *glossy* prints of photos should be submitted. Lettering should be neat, and designed for the reduction anticipated. Please include a separate list of captions.
6. Formulas should be expressed as simply as possible, keeping in mind the difficulties and limitations encountered in setting type.